

# Effects of spin-wave excitations in half-metallic materials

N. H. Long,<sup>1,2,\*</sup> M. Ogura,<sup>2</sup> and H. Akai<sup>2</sup><sup>1</sup>*Peter Grünberg Institut and Institute for Advanced Simulation, Forschungszentrum Jülich and JARA, D-52425 Jülich, Germany*<sup>2</sup>*Department of Physics, Graduate School of Science, Osaka University, 1-1 Machikaneyama, Toyonaka 560-0043, Japan*

(Received 10 October 2011; published 28 June 2012)

Finite-temperature magnetic properties of half-metallic materials are investigated on the basis of the first-principles Korringa-Kohn-Rostoker Green's function method. Influences of spin-wave excitations on the electronic structure are examined in the framework of the coherent potential approximation. The calculations show that the half-metallicity is easily destroyed due to an appearance of low-energy electron excited states in the minority-spin band gap at finite temperature. On the other hand, calculated dc conductivity shows that the 100% spin-polarized conduction occurring in half-metallic materials hardly deteriorates even in such a temperature.

DOI: [10.1103/PhysRevB.85.224437](https://doi.org/10.1103/PhysRevB.85.224437)

PACS number(s): 75.30.Ds, 75.76.+j, 75.47.Np

## I. INTRODUCTION

Half-metallic materials, which are metallic in one spin direction while insulating in the other spin direction, have attracted much attention not only due to their unique property but also due to their possible applications in spintronics.<sup>1</sup> For instance, the magnetoresistance ratio of giant magnetoresistance (GMR) and tunneling magnetoresistance (TMR) devices using half-metallic materials is supposed to remarkably increase because of their 100% spin-polarized Fermi surfaces. Such applications, however, have not yet appeared until now.

One obstacle that prevents practical applications of the half-metallic materials is temperature effects: First, many half-metals have a rather low magnetic transition temperature, such as 180 K for (Ga, Mn)As half-metallic diluted magnetic semiconductors.<sup>2</sup> This problem, however, has been largely eased since the appearance of a family of Co<sub>2</sub>YZ-type Heusler alloys, which include half-metals with a high magnetic transition temperature.<sup>3</sup> Some of these half-metallic ferromagnets, in fact, show a Curie temperature  $T_C$  much higher than room temperature (RT), for example, 1100 K of Co<sub>2</sub>FeSi (Ref. 4).

Yet another temperature effect is the following. Several experimental groups have succeeded in fabricating magnetic tunneling junctions (MTJs) consisting of the above Heusler alloys.<sup>5-9</sup> In their works, Sakuraba *et al.* showed that an MTJ consisting of Co<sub>2</sub>MnSi as a bottom electrode, Al-O as a tunneling barrier, and Co<sub>0.75</sub>Fe<sub>0.25</sub> as a top electrode exhibits 159% TMR ratio and 89% spin polarization at 2 K.<sup>7</sup> However, the TMR ratio of the MTJ rapidly decreased to 70% at RT. In addition, Wang *et al.* observed only 12% spin polarization of Co<sub>2</sub>MnSi films at RT.<sup>8</sup> Similarly, Yamamoto *et al.* found that a high TMR ratio of 192% at 4.2 K for a Co<sub>2</sub>MnSi/MgO/CoFe MTJ decreased considerably to 90% at RT.<sup>9</sup>

Although the decrease in the TMR ratios at RT has often been attributed to an effect of disorder,<sup>10</sup> Chioncel *et al.* proposed an idea of appearance of non-quasiparticle (NQP) states such as magnons in the insulator gap.<sup>11,12</sup> It would destroy the half-metallicity at a finite temperature and hence might reduce the TMR ratio. In their study, the dynamical spin fluctuations at finite temperature were investigated in a many-body approach, that is, dynamical mean-field theory (DMFT) combined with the local density approximation (LDA) of the density functional theory (DFT). Their results for Co<sub>2</sub>MnSi showed that tail parts of the NQP states at

200 K and 400 K crossed the Fermi energy and contributed to the depolarization of the Fermi surfaces. Thoene *et al.* also calculated magnon dispersion relations of half-metallic Heusler alloys using an approach based on the Korringa-Kohn-Rostoker (KKR) Green's function method combined with the Heisenberg model.<sup>13</sup> However, they mentioned little about the half-metallicity that may deteriorated due to the magnon excitations.

In this paper, we investigate the effects of spin-wave (magnon) excitations in half-metals using an approach different from that of the above authors. A basic quantity in which we are interested is the retarded Green's function at temperature  $T$  defined by

$$iG = \text{Tr}[\exp(-\beta H)\{\varphi(r, t), \varphi^\dagger(r', t')\}\theta(t - t')], \quad (1)$$

where  $\beta = 1/T$ ,  $\varphi$  is the electron annihilation operator, and  $\theta$  is the step function. Neglecting the time fluctuations (static approximation), we may approximate the expression as

$$iG \simeq Z^{-1} \int \mathcal{D}[V(r)] \exp\{-\beta \Psi[V(r), \beta]\} \hat{G}[V(r)]. \quad (2)$$

Here,  $\hat{G}[V(r)]$  is the noninteracting retarded Green's function in an external field  $V(r)$ ,  $\Psi[V(r)]$  is the free energy for the corresponding system, and  $\int \mathcal{D}[V(r)]$  stands for the functional integral with respect to  $V(r)$ .  $Z$  is the partition function defined by

$$Z = \int \mathcal{D}[V(r)] \exp\{-\beta \Psi[V(r), \beta]\}. \quad (3)$$

Further approximation is needed to perform the functional integrals appearing in Eqs. (2) and (3). Since the functional integral is nothing but a configurational average of a quantity with respect to the external potential  $V(r)$ , a simple and yet feasible approximation is the coherent potential approximation (CPA) that takes the configurational average within the single-site approximation. The probability of finding a particular potential is now given by  $Z^{-1} \exp(-\beta \Psi)$ . This quantity  $\Psi$  is determined if  $G$  is known. Therefore, these procedures form a self-consistent loop with respect to the concentration of a particular  $V$ . Also, the continuous variations of the potential  $V$  have to be taken. In the present study we employ the following scheme: We take only the potential that gives a local minimum of  $\Psi$  for each direction of the local magnetic moment; that

is, we employ a saddle-point approximation. Furthermore, the probability of finding the local potential is obtained from an independent procedure: First, the magnetic exchange coupling constants  $J_{ij}$  are calculated in the framework of the KKR Green's function method. This procedure maps the LDA Kohn-Sham Hamiltonian to a Heisenberg model. Then, using a cluster approximation, the temperature dependence of magnetization of the system is obtained. This enables us to estimate the average number of flipped spins (*wrong spins*) at a finite temperature. We then identify the probability of finding flipped and nonflipped spins as  $\exp(-\beta\Psi)$ .

This procedure is equivalent to the procedure in which spins are regarded as randomly distributed static local moments and the electronic structure is calculated by use of the CPA in the framework of the KKR Green's function method. The conductivity is calculated similarly using the KKR-CPA combined with Kubo-Greenwood formula.

In the present study, not only Heusler alloys but also half-metallic antiferromagnets (HM-AF),<sup>14,15</sup> which have a high magnetic transition temperature and also form a stable chemical ordered state, are examined with applications to spintronic devices in mind.

## II. THEORY

### A. Mano cluster approximation

A simple systematic cluster approximation which is suitable for both concentrated and diluted magnetic alloys was proposed by Mano in 1977<sup>16</sup> and was applied to half-metals by Ogura *et al.*<sup>17</sup> We briefly review the formulation in the following.

Consider a Heisenberg model whose effective Hamiltonian is given by

$$H = -2 \sum_{(i,j)} J_{ij} \mathbf{e}_i \cdot \mathbf{e}_j. \quad (4)$$

Here,  $\mathbf{e}_i$  denotes the unit vector in the direction of the local magnetic moment of site  $i$ ;  $J_{ij}$  is the magnetic exchange parameter. The normalized magnetization of the system is given by

$$M = \text{Tr} \left[ \left( \sum_{i=1}^N \mathbf{e}_i^z \right) \rho \right], \quad (5)$$

where  $\rho$  is the density matrix given by

$$\rho = \frac{e^{-\beta H}}{\text{Tr} e^{-\beta H}}, \quad (6)$$

where  $\beta = 1/k_B T$  and  $N$  is the total number of magnetic ions in the system. We define the order parameter  $m = \langle e_i^z \rangle$ , where  $\langle e_i^z \rangle$  is the average normalized magnetization  $M/N$ .

We employ a one-site approximation where  $m$  is approximated by

$$m = \text{Tr}[e_1^z \rho_1], \quad (7)$$

where  $\rho_1$  is the density matrix for the site 1. We give the density matrix in which the fluctuation of the effective field is taken into account. In Eq. (4), we replace those spin operators except  $\mathbf{e}_1$  with stochastic variables such that  $e_i^x = e_i^y = 0$  and  $e_i^z = \sigma_i$ . The valuable  $\sigma_i$  is assumed to take the value  $+1$  or  $-1$ . In the

following, for simplicity, we take only the nearest-neighbor interactions into account and suppose  $J_{ij} = J$  for all nearest-neighbor couplings. The one-site effective Hamiltonian is thus obtained as

$$H_{1,\sigma} = -2J \sum_i e_1^z \sigma_i = -h_{1,\sigma} e_1^z \quad (8)$$

and the density matrix is given by

$$\rho_{1,\sigma} = \frac{e^{-\beta H_{1,\sigma}}}{\text{Tr} e^{-\beta H_{1,\sigma}}}. \quad (9)$$

Equation (7) is calculated by taking the average of  $\text{Tr}[e_1^z \rho_{1,\sigma}]$  over all the possible configurations of  $\{\sigma_i\}$ , which is a set of  $\sigma_i$ 's at the nearest neighbors of the site 1:

$$m = \langle \text{Tr}[e_1^z \rho_{1,\sigma}] \rangle_\sigma. \quad (10)$$

The average  $\langle \cdots \rangle_\sigma$  is calculated when the probability distribution function  $P(\{\sigma_i\})$  is given. Here we approximate  $\sigma_i$  to be independent of one another and the average of each  $\langle \sigma_i \rangle_\sigma$  to be equal to  $m$ . Then  $P(\{\sigma_i\})$  is expressed as a product of single distribution functions  $P(\sigma_i)$ , which is written as

$$P(\sigma_i) = \delta(\sigma_i - 1) \frac{1+m}{2} + \delta(\sigma_i + 1) \frac{1-m}{2}. \quad (11)$$

We assume the classical spin description for  $e_1^z$ . In this case,

$$\text{Tr}[e_1^z \rho_{1,\sigma}] = \frac{\int_{-1}^1 x e^{\beta h_{1,\sigma} x} dx}{\int_{-1}^1 e^{\beta h_{1,\sigma} x} dx} = L(\beta h_{1,\sigma}), \quad (12)$$

where  $L(x)$  is the Langevin function,  $L(x) = \coth x - 1/x$ . When there are  $n$  sites located around the site 1, and  $k$  among them have  $\sigma_i = -1$  and the rest  $\sigma_i = +1$ ,  $h_{1,\sigma} = 2J(n - 2k)$ . The probabilities of finding such a spin configuration are given by binomial distributions:

$$D_k^n = \binom{n}{k} \left( \frac{1+m}{2} \right)^{n-k} \left( \frac{1-m}{2} \right)^k. \quad (13)$$

Thus, we obtain the self-consistent equation for  $m$ :

$$m = \sum_{k=0}^n D_k^n L(2\beta J(n - 2k)). \quad (14)$$

From Eq. (14), the temperature dependence of the magnetization of the system is calculated.

In the KKR Green's function method, following the prescription of Liechtenstein *et al.*,<sup>18</sup>  $J_{ij}$  is obtained as

$$J_{ij} = \frac{1}{4\pi} \int_{-\infty}^{E_F} dE \Im \text{Tr}[\Delta_i \tau_{\uparrow}^{ij} \Delta_j \tau_{\downarrow}^{ji}], \quad (15)$$

where  $\Delta_i$  denotes the difference in the inverse single-site scattering matrices ( $t$ -matrices) for spin-up and spin-down states.  $\tau$  is the scattering path operator.

### B. Kubo-Greenwood formula

To discuss the effect of spin-wave excitations in GMR/TMR devices, the conductivity of the system is calculated by using the Kubo-Greenwood formula combined with the KKR Green's function method. For the details of the calculations, we refer to Ref. 19. The same method was also used to study the

transport properties of half-metallic systems.<sup>20,21</sup> The general expression for the conductivity is summarized as follows.

The diagonal parts of conductivity tensor along the  $z$  direction is obtained by

$$\sigma_{zz}(\epsilon) = \frac{\pi\hbar}{V} \left\langle \sum_{\alpha, \alpha'} \langle \alpha | j_z | \alpha' \rangle \langle \alpha' | j_z | \alpha \rangle \delta(\epsilon - \epsilon_\alpha) \delta(\epsilon - \epsilon_{\alpha'}) \right\rangle, \quad (16)$$

where  $j_z$  is the current operator,

$$j_z = -i\hbar \frac{e}{m} \frac{\partial}{\partial z}, \quad (17)$$

and  $V$  is the volume of the system. The quantum states  $|\alpha\rangle$ 's represent the eigenstates of a particular configuration of the random system. The large bracket indicates that an average over configurations is to be taken. Equation (16) can be rewritten in terms of Green's function as

$$\sigma_{zz}(\epsilon) = \frac{1}{4} \lim_{\eta \rightarrow 0} [\tilde{\sigma}_{zz}(\epsilon + i\eta, \epsilon + i\eta) + \text{c.c.}] - \tilde{\sigma}_{zz}(\epsilon + i\eta, \epsilon - i\eta) - \text{c.c.}], \quad (18)$$

where

$$\tilde{\sigma}_{zz}(z, z') = -\frac{\hbar}{\pi V} \text{Tr}(j_z G(z) j_z G(z')). \quad (19)$$

For disordered systems, the configuration average can be taken approximately in the framework of CPA.

A small but finite imaginary part  $i\eta$  (here we take  $\eta = 10^{-6}$ ) is added to the Fermi energy in using the Kubo-Greenwood formula. For this reason, even in an ordered structure where no scattering due to disorder arises, the conductivity for metallic bands remains finite. dc conductivity is given by  $\sigma_{zz}(E_F)$ , where  $E_F$  is the Fermi energy.

### III. RESULTS AND DISCUSSIONS

#### A. The disappearance of band gap by spin-wave excitations

In Fig. 1, the order parameter  $m$ , which is the ratio of the magnetic moment at temperature  $T$  to that at 0 K of Mn in  $\text{Co}_2\text{MnSi}$  Heusler alloys, is shown as a function of reduced

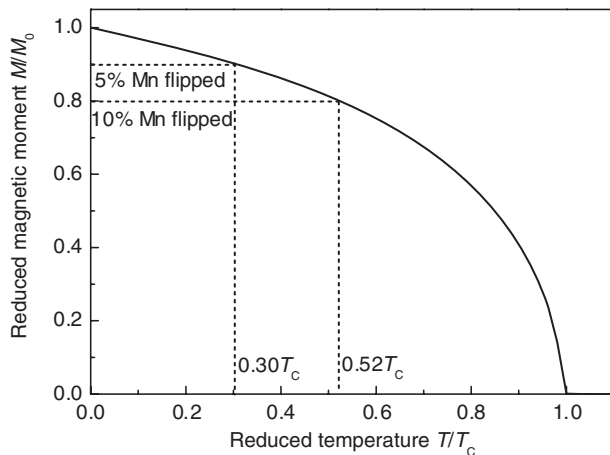


FIG. 1. The dependence on temperature of magnetic moment of Mn in  $\text{Co}_2\text{MnSi}$  half-metallic Heusler alloys.

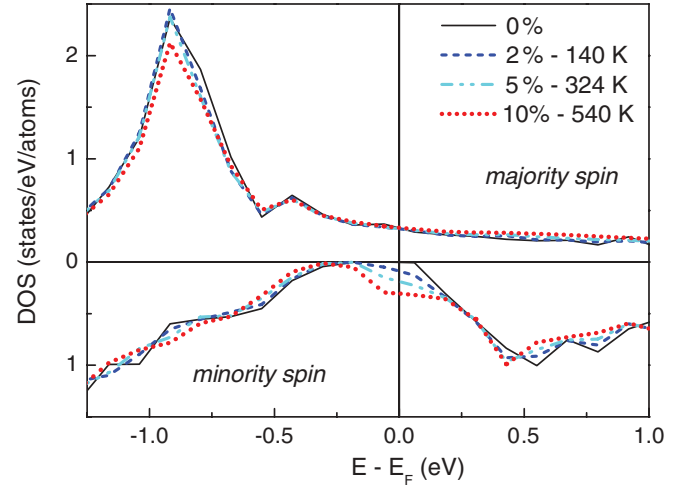


FIG. 2. (Color online) Density of states of  $\text{Co}_2\text{MnSi}$  Heusler alloys with some percentages of wrong-spin Mn.

temperature  $T/T_C$ . Here, the calculated magnetic transition temperature  $T_C$  is 1080 K, which is comparable with the experimental value of 985 K.<sup>22</sup> It can be seen in Fig. 1 that the magnetic moment of Mn is 90% of that at  $T = 0$  (hereafter  $M_0$ ) at  $0.30T_C$ , while it is 80% of  $M_0$  at  $0.52T_C$ . Our  $M-T$  curve is very similar to that given by Sasioglu *et al.* in the classical limit.<sup>23</sup>

To take the existence of these spin-wave excitations into account, we take the following model system. Let us consider the system at  $0.30T_C$ . The total magnetic moment of Mn in this system is 90% of  $M_0$ . It corresponds to a system in which 5% of Mn atoms have a wrong direction of the local magnetic moment (say, down) against other Mn atoms with the correct direction (up) of the moment. Therefore, this system might be simulated by introducing 5% Mn with spin-down magnetic moment randomly in an otherwise spin-up magnetic moment. This configuration can be treated easily in the framework of CPA by considering a random alloy system whose composition is expressed as  $\text{Co}_2(\text{Mn}_{0.95}^{\uparrow}\text{Mn}_{0.05}^{\downarrow})\text{Si}$ . The concentration of spin-flipped atoms in the sample is decided from the magnetization at finite temperature and hence depends on the temperature of the system.

In Fig. 2, the total densities of states (DOS) of spin-existed states with 2%, 5%, and 10% wrong-spin Mn (i.e., Mn atoms with a wrong direction of the local magnetic moment), corresponding to the system at 140 K, 324 K, and 540 K, respectively, are shown. It is clearly seen that existence of even a small percentage of wrong-spin Mn is enough to destroy the half-metallicity. The band gap disappears due to the formation of  $d$  state of wrong-spin Mn at the Fermi energy in the spin-down bands. Accordingly, the magnitude of the DOS at the Fermi energy in the spin-down band increases with increasing the concentration of wrong-spin Mn.

Our results in Fig. 2 calculated by LDA combined with CPA show a good correspondence with Fig. 1 of Ref. 12 calculated by LDA + DMFT. We may also say that the effect of spin-wave excitations studied here seems much stronger than the spin-orbit coupling effect.

A similar approach is applied to NiAs-type  $(\text{FeCr})\text{Se}_2$ , which were predicted to be HM-AF by the present authors.<sup>14,15</sup>

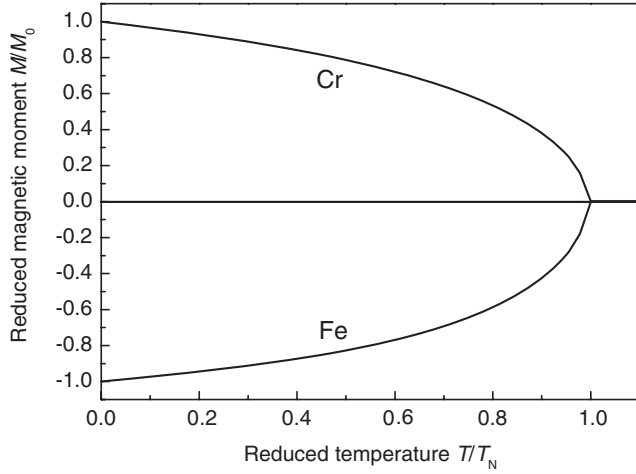


FIG. 3. The dependence on temperature of magnetic moments of Cr and Fe in half-metallic antiferromagnets NiAs-type  $(\text{FeCr})\text{Se}_2$ .

In Fig. 3, the order parameters of magnetic moments of Cr and Fe are shown as a function of reduced temperature. In this system, the magnetic coupling between Cr and Fe is antiferromagnetic. We assume the magnetic moment of Cr to be positive and that of Fe to be negative. The calculated  $T_N$  is 895 K.

To examine the electronic structure of spin excited states, we introduce the atoms with wrong spin at Fe and Cr sites. The composition of such system is now expressed as  $(\text{Fe}_{1-x}^\downarrow\text{Fe}_x^\uparrow)(\text{Cr}_{1-x}^\uparrow\text{Cr}_x^\downarrow)\text{Se}_2$ . Figure 4 displays the DOS of systems for  $x = 2\%$ ,  $5\%$ , and  $10\%$ . As can be seen in the figure, though such half-metals have large band gap near Fermi level in the spin-down band at 0 K, the band gap is diminished by the  $d$  states of spin-flipped atoms at finite temperature, such as the case of Heusler alloys. The magnitude of the DOS at the Fermi energy in the spin-down band also increases with increasing the concentration of spin-flipped atoms.

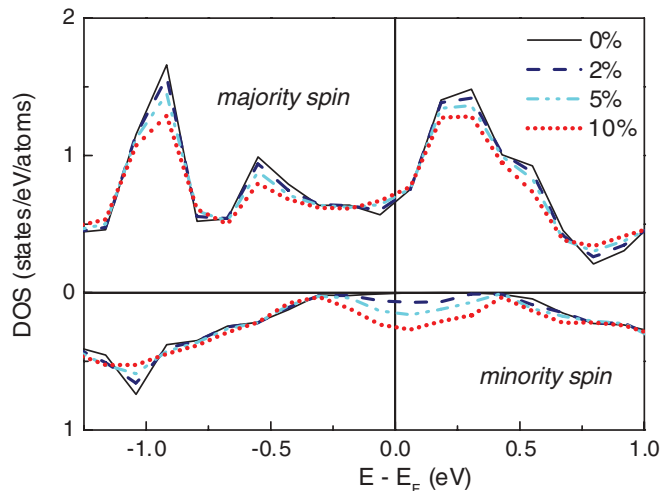


FIG. 4. (Color online) DOS of  $(\text{Fe}_{1-x}^\downarrow\text{Fe}_x^\uparrow)(\text{Cr}_{1-x}^\uparrow\text{Cr}_x^\downarrow)\text{Se}_2$  with  $x = 2\%$ ,  $5\%$ ,  $10\%$ .

## B. Effects of the spin-wave excitations on the transport properties

In the previous section, we saw that the half-metallicity was destroyed by spin-wave excitations. In this section, spin-decomposed dc conductivity of the system is calculated using the Kubo-Greenwood formula combined with KKR-CPA. By comparing the ratio of the conductivity of the spin-up channel to that of the spin-down channel, the effects of spin-wave excitations on transport properties of half-metals are examined.

Here, it might be worth noticing that there is no direct relationship between the conductivity and the density of states at the Fermi energy, particularly in the case of systems containing transition-metal elements. When the Fermi surfaces have  $d$  components, it is not generally true that a high density of state corresponds to a high conductivity, which might be expected in the case that the Fermi surfaces are mostly composed of  $s$  and  $p$  components. On the contrary, the high density of states often leads to a very low conductivity in these cases. It is because the high density of  $d$  states means a low electron velocity due to its large effective mass. Moreover,  $d$  states are strongly affected by existing disorder because of a  $d$  resonance scattering. Under such circumstances, the conductivity is strongly suppressed.

It is naturally supposed that most of the states which appear due to the spin-wave excitations at the Fermi energy in the spin-down band is contributed by the  $d$  states of transition metal atoms with wrong spin. Therefore, it is expected that the conductivity in the spin-down channel cannot be high. Figure 5 shows the conductivity for each spin band of  $\text{Co}_2\text{MnSi}$  with 2% spin-flipped sites as a function of energies relative to the Fermi energy. It is recognized that the conductivity of the spin-down bands at Fermi energy, which has a value of  $0.346 \text{ k}\Omega^{-1} \text{ cm}^{-1}$ , is much smaller than  $66 \text{ k}\Omega^{-1} \text{ cm}^{-1}$  of the spin-up bands.

In Fig. 6 we show the conductivity in the spin-up and -down channels of  $\text{Co}_2\text{MnSi}$  at various percentages of wrong-spin Mn ranging from 1% to 25%. As seen in this

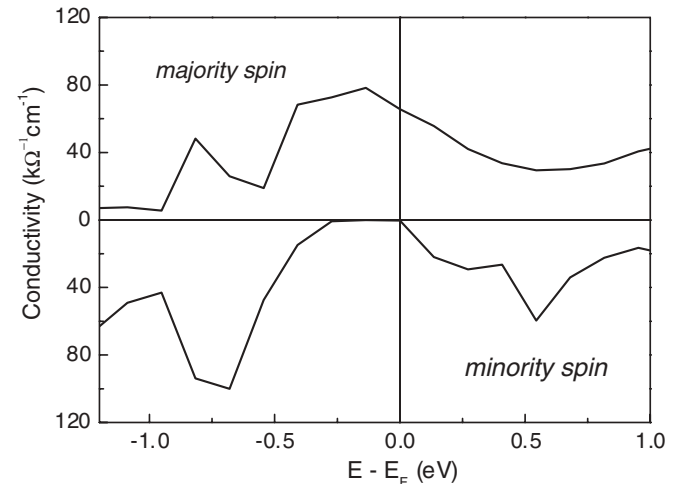


FIG. 5. Conductivity of  $\text{Co}_2\text{MnSi}$  with 2% spin-flipped atoms as a function of fictitious Fermi energy.



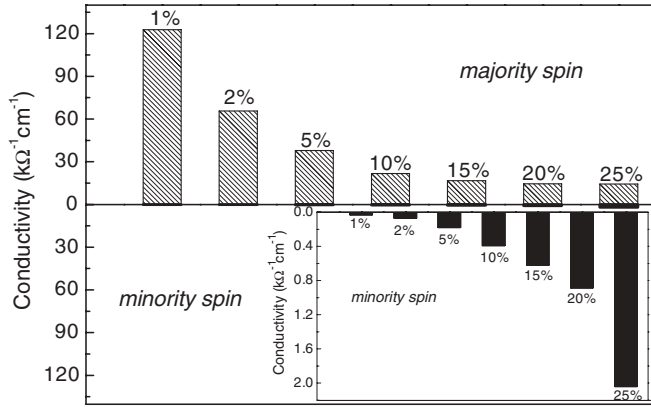


FIG. 6. Conductivity of up- and down-spin channels of Co<sub>2</sub>MnSi with various percentages of wrong-spin states. The inset is an enlarged figure for the spin-down band.

figure, the conductivity of the spin-up band is much larger than that of the spin-down band, the latter being almost invisible. The inset is an enlarged figure of the conductivity for the spin-down band. The conductivity of the spin-up band decreases and the conductivity of the spin-down band increases with increasing concentration of spin-flipped atoms. Thus, the ratio of conductivity between spin-up and -down bands decreases with increasing the concentration of wrong-spin Mn. However, the ratio remains huge even at 25% spin-flipped Mn atoms. It is noticeable that the temperature corresponds to 25% spin-flipped Mn atoms is around 850 K or  $0.85T_C$ .

The calculated conductivity is comparable with that seen in experiments. In the present model, 1%, 2%, and 5% spin-flip Mn atoms correspond to around 80 K, 140 K, and 324 K, respectively. The resistivity at these temperatures is about  $8 \mu\Omega\text{cm}$ ,  $15 \mu\Omega\text{cm}$ ,  $26 \mu\Omega\text{cm}$  in the calculation and around  $8 \mu\Omega\text{cm}$ ,  $11 \mu\Omega\text{cm}$ ,  $21 \mu\Omega\text{cm}$  in experiments,<sup>24</sup> respectively. Since the present calculation gives residual resistivity, calculated values should be a little smaller than experimental ones. Although the calculated values are larger than experiments, these are comparable and the present model seems to provide good estimation.

The same observation is also obtained for HM-AF (FeCr)Se<sub>2</sub>. Figure 7 shows the conductivity of the spin-up and -down channels of (FeCr)Se<sub>2</sub> up to 25% of wrong-spin sites. The conductivity of the spin-up band is very large and the ratio of the conductivity of the spin-up band to that of the spin-down band is also very large, even in a system with a rather high percentage of wrong-spin states. As a consequence, the spin-wave excitations at finite temperature seem not to much affect the transport properties of these half-metals.

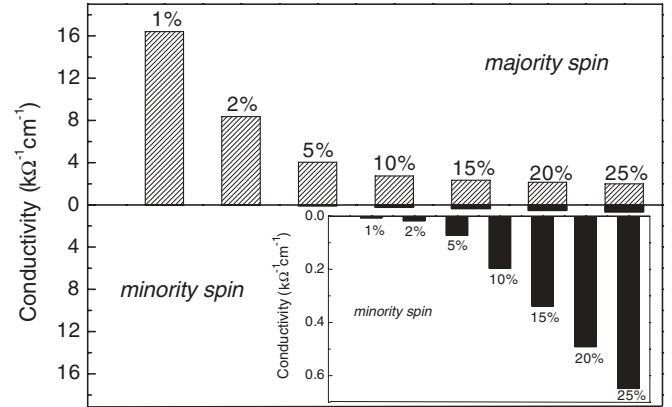


FIG. 7. Conductivity of up- and down-spin channels of NiAs-type (FeCr)Se<sub>2</sub> with various percentages of wrong-spin states. The inset is an enlarged figure for the spin-down band.

#### IV. SUMMARY

The effect of spin-wave excitations in half-metals at finite temperature was investigated using the first-principles KKR-CPA method on an assumption that these excitations can be described by randomly distributed local-moment reversals. The number of reversed local moments at a given temperature was determined by the Mano cluster approximation applied to a Heisenberg-type Hamiltonian obtained through Liechtenstein's prescription. These procedures were exploited for HM ferromagnetic Co<sub>2</sub>MnSi and HM antiferromagnetic (FeCr)Se<sub>2</sub>. The results indicated that the spin-wave excitations easily destroyed the half-metallicity even at a rather low temperature  $\sim 0.1T_C$  ( $T_N$ ). This effect is much stronger than the other effects such as spin-orbit coupling, which also is a reason for the destruction of the half-metallicity. Nevertheless, the spin polarization in the conductivity, which was calculated by the Kubo-Greenwood formula combined with KKR-CPA method, was little affected by the spin-wave excitations in these half-metallic materials. This is due to the fact that the states that are produced by the local-moment reversal form a rather localized impurity band that is similar to a band composed of virtual bound states. These states cause a strong  $d$  scattering and hence contribute little to electron conduction. The large magnetoresistance effect, therefore, should be quite robust if half-metals are used in GMR/TMR devices.

#### ACKNOWLEDGMENTS

This work was supported by the Next Generation Super Computing Project, Nanoscience Program, MEXT, Japan, and by MEXT KAKENHI No. 17064008.

\*h.nguyen@fz-juelich.de

<sup>1</sup>I. Zutic, J. Fabian, and D. Sarma, *Rev. Mod. Phys.* **76**, 323 (2004).

<sup>2</sup>H. Ohno, *Science* **281**, 591 (1998).

<sup>3</sup>C. Felser and B. Hillebrands, *J. Phys. D: Appl. Phys.* **42**, 080301 (2009).

<sup>4</sup>S. Wurmehl, G. H. Fecher, H. C. Kandpal, V. Ksenofontov, C. Felser, and H. J. Lin, *Appl. Phys. Lett.* **88**, 032503 (2006).

- <sup>5</sup>M. Yamato, T. Marukame, T. Ishikawa, K. Matsuda, T. Uemura, and M. Arita, *J. Phys. D: Appl. Phys.* **39**, 824 (2006).
- <sup>6</sup>Y. Sakuraba, M. Hattori, M. Oogane, Y. Ando, H. Kato, A. Sakuma, T. Miyazaki, and H. Kubota, *Appl. Phys. Lett.* **88**, 192508 (2006).
- <sup>7</sup>Y. Sakuraba, T. Miyakoshi, M. Oogane, Y. Ando, A. Sakuma, and T. Miyazaki, *Appl. Phys. Lett.* **89**, 052508 (2006).
- <sup>8</sup>W. H. Wang, M. Przybylski, W. Kuch, L. I. Chelaru, J. Wang, Y. F. Lu, J. Barthel, H. L. Meyerheim, and J. Kirschner, *Phys. Rev. B* **71**, 144416 (2005).
- <sup>9</sup>T. Ishikawa, T. Marukame, H. Kijima, K. I. Matsuda, T. Uemura, M. Arita, and M. Yamamoto, *Appl. Phys. Lett.* **89**, 192505 (2006).
- <sup>10</sup>V. Jung, G. H. Fecher, B. Balke, V. Ksenofontov, and C. Felser, *J. Phys. D: Appl. Phys.* **42**, 084007 (2009).
- <sup>11</sup>L. Chioncel, M. I. Katsnelson, G. A. de Wijs, R. A. de Groot, and A. I. Liechtenstein, *Phys. Rev. B* **71**, 085111 (2005).
- <sup>12</sup>L. Chioncel, Y. Sakuraba, E. Arrigoni, M. I. Katsnelson, M. Oogane, Y. Ando, T. Miyazaki, E. Burzo, and A. I. Liechtenstein, *Phys. Rev. Lett.* **100**, 086402 (2008).
- <sup>13</sup>J. Thoene, S. Chadov, G. H. Fecher, C. Felser, and J. Kübler, *J. Phys. D: Appl. Phys.* **42**, 084013 (2009).
- <sup>14</sup>H. Akai, M. Ogura, and N. H. Long (to be published).
- <sup>15</sup>N. H. Long, M. Ogura, and H. Akai, *J. Phys.: Condens. Matter* **21**, 064241 (2009).
- <sup>16</sup>H. Mano, *Prog. Theor. Phys.* **57**, 1848 (1977).
- <sup>17</sup>M. Ogura, C. Takahashi, and H. Akai, *J. Phys.: Condens. Matter* **19**, 365226 (2007).
- <sup>18</sup>A. I. Liechtenstein, M. I. Katsnelson, V. P. Antropov, and V. A. Gubanov, *J. Magn. Magn. Mater.* **67**, 65 (1987).
- <sup>19</sup>W. H. Butler, *Phys. Rev. B* **31**, 3260 (1985).
- <sup>20</sup>H. Akai and M. Ogura, *J. Phys. D: Appl. Phys.* **40**, 1238 (2007).
- <sup>21</sup>N. H. Long and H. Akai, *J. Supercond. Novel Magn.* **20**, 473 (2007).
- <sup>22</sup>P. J. Webster, *J. Phys. Chem. Solids* **32**, 1221 (1971).
- <sup>23</sup>E. Sasioglu, L. M. Sandratskii, P. Bruno, and I. Galanakis, *Phys. Rev. B* **72**, 184415 (2005).
- <sup>24</sup>L. Ritchie, G. Xiao, Y. Ji, T. Y. Chen, C. L. Chien, M. Zhang, J. Chen, Z. Liu, G. Wu, and X. X. Zhang, *Phys. Rev. B* **68**, 104430 (2003).